STRATOSPHERIC OClO AND BrO PROFILES FROM SCIAMACHY LIMB MEASUREMENTS

Sven Kühl [1], Janis Pukite [1], Tim Deutschmann [2], Marcel Dorf [2], Francois Hendrick [3], Ulrich Platt [2] and Thomas Wagner [1]

1) Max Planck Institut für Chemie, Mainz, JJBW 27, 55128 Mainz, Germany
2) Institut für Umweltphysik, University of Heidelberg, INF 229, 69120 Heidelberg, Germany
3) Belgian Institute for Space Aeronomy, 1180 Brussels, Belgium
E-mail: Sven.Kuehl@mpch-mainz.mpg.de

ABSTRACT

From the limb viewing geometry (i.e. tangential to Earth's surface and its atmosphere) it is possible to retrieve moderate resolution vertical profiles of various stratospheric trace gases. BrO and OClO profiles retrieved from the SCIAMACHY Limb measurements in a two step approach are presented and compared to independent groundbased, balloon borne and satellite observations. For the BrO profiles, a good agreement is found. For OClO profiles, there exist no correlative validation measurements so far. However, since OClO is an indicator for ClO, the OClO profiles derived from SCIAMACHY limb observations are compared to measurements of ClO by AURA-MLS and ODIN-SMR. Also, the effect of horizontal gradients in the trace gas distribution on the profile retrieval is investigated.

1. STRATOSPHERIC CHLORINE AND BROMINE ACTIVATION

In the polar winter, stratospheric temperatures can fall below the threshold for formation of polar stratospheric clouds (PSCs). On PSC particles, heterogeneous reactions take place, which convert the ozone-inert chlorine reservoirs (mainly $ClONO_2$ and HCl) into ozone destroying species (active chlorine, mainly Cl, ClO and ClOOCl, see e.g. [1]). This activation of chlorine initiates catalytic ozone destruction cycles like the ClO-ClOOCl and the ClO-BrO cycle [2,3]. OClO (chlorine dioxide) is almost exclusively formed by reaction of ClO with BrO [4]. The amount of OClO in an air mass therefore gives a good indication of the level of chlorine activation, especially for solar zenith angles below 90 degrees [5,6,7]. Since OClO shows strong differential absorption features in the UV spectral range, it can be detected by means of Differential Optical Absorption Spectroscopy (DOAS) [8,9,10]. Nadir observations of OClO by GOME [17], the predecessor of SCIAMACHY, have been applied for the long-term monitoring of chlorine activation [10,11,12] and for case studies [13,14,15].
Also for bromine, activation from the reservoirs to the active compounds takes place during polar winter. However, a large fraction of stratospheric bromine is in its active form already under normal conditions (while 95% of stratospheric chlorine is stored in the reservoirs HCl and $ClONO_2$ under "non-polar winter" conditions). Both halogen species cause chemical destruction of ozone in polar spring, leading to the well-known ozone hole over Antarctica [1]. Moreover, also at mid-latitudes and equatorial regions a negative trend of the ozone column is observed, which is attributed to transport mechanisms and halogen chemistry.
Until the launch of SCIAMACHY, vertical profiles of BrO and OClO have not been measured on a long term and global scale. Compared to observations of total columns, the knowledge about the vertical distribution of trace gases allows to establish correlations between them (and to meteorological parameters) in a much more quantitative manner and also on individual altitude levels. Thus, limb measurements of scattered sunlight provide a new insight in stratospheric chemistry and are valuable to investigate still open questions.

2. SCIAMACHY LIMB MEASUREMENTS

The Scanning Imaging Absorption Spectrometer for Atmospheric Chartography [16] is a UV/VIS/NIR grating spectrometer aboard the European Environmental satellite ENVISAT-1. The satellite operates in a near polar Sun synchronous orbit with inclination from the equatorial plane of approximately 98.5°. It performs one orbit in 100 minutes with equator crossing time of 10:00 in descending mode.
SCIAMACHY measures the intensities of the direct sunlight and of the light scattered back from the earth and its atmosphere in moderate spectral resolution over a wide wavelength range in nadir, limb and occultation viewing modes. At the day side of Earth the instrument probes the atmosphere in alternating sequences of nadir and limb measurements. The Limb scans are performed with approximately 3.3 km altitude steps from ground to approx. 100 km height. Horizontally the atmosphere is scanned with swaps across flying direction of 960 km at tangent point, consisting of 4 pixels with 240 km width each, see Fig. 1. The instantaneous field of view is 0.045° in elevation and 1.8° in azimuth, which corresponds to approximately 2.5 km and 110 km at the tangent point respectively.

Proceedings of the Third Workshop on the Atmospheric Chemistry Validation of Envisat (ACVE-3)
4-7 December 2006, ESRIN, Frascati, Italy (ESA SP-642,February 2007)

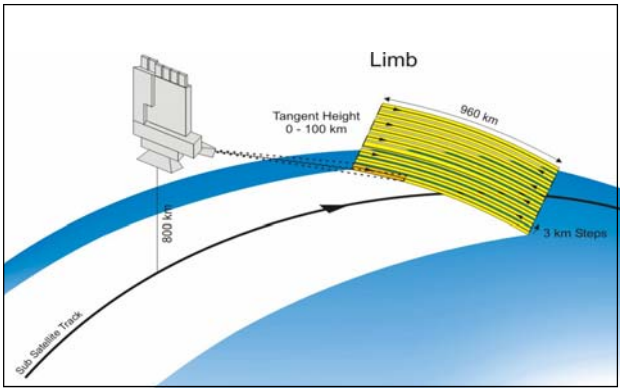

Figure 1: *SCIAMACHY limb geometry.*

SCIAMACHY is measuring spectra in the UV-VIS-NIR range from 240 to 2380 nm, allowing the retrieval of a variety of trace gases [16]. In the UV/VIS, the spectral resolution ranges between approximately 0.25 – 0.55 nm which is sufficient to perform Differential Optical Absorption Spectroscopy (DOAS, see [9]) of e.g. Ozone, NO_2, BrO and OClO.

As example, Fig. 2 shows intensities measured by SCIAMACHY in the UV spectral region at different selected elevation angles, corresponding approximately to the altitudes stated. It can be seen that the intensity increases by orders of magnitude when scanning from 40 km altitude downwards to ground-level. This is due to the larger density of air molecules for low altitudes resulting in a higher probability for scattering processes. The high frequent structure of the spectra arises from the Fraunhofer lines, with the most prominent ones at 393.36 and 396.84 nm. For altitudes between 40 and 20 km, the absorption by the ozone layer can bee seen very nicely for wavelengths below 330 nm. To determine also the absorption of weaker absorbers, it requires advanced techniques like DOAS.

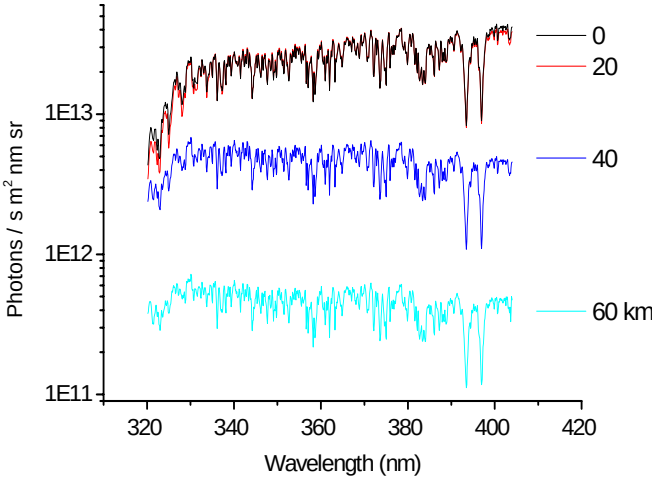

Figure 2: *Examples for SCIAMACHY limb spectra in the UV, measured at different selected elevation angles corresponding approximately to the altitudes stated.*

3. RETRIEVAL OF VERTICAL PROFILES

For the profile retrieval we use a two step approach: First, Slant Column Densities (SCDs) of the respective absorber are determined in the UV/VIS spectral range by DOAS. Second, inversion of the retrieved SCDs (as function of tangent height) yields vertical profiles of the trace gas concentration (as function of altitude). For that purpose, we either apply an optimal estimation method (constraining the inversion by a priori information) or invert the measurements by a least squares approach (independently from a priori). For both approaches box air mass factors calculated by the full spherical radiative transfer model (RTM) TRACY-II [26] are utilized as weighting functions.

Figure 3 gives a schematic overview of the two step approach. The blue boxes represent the first part of the retrieval with the first row summarizing the parameters that are used as input for this step. The yellow boxes symbolize the calculations by the RTM Tracy II. Again, the first row consists of the input parameters for the RTM. Finally, the green boxes stand for the second step, the inversion to profiles, in which the constraint by a priori knowledge can be optionally applied. In the following, the two retrieval steps are described in detail.

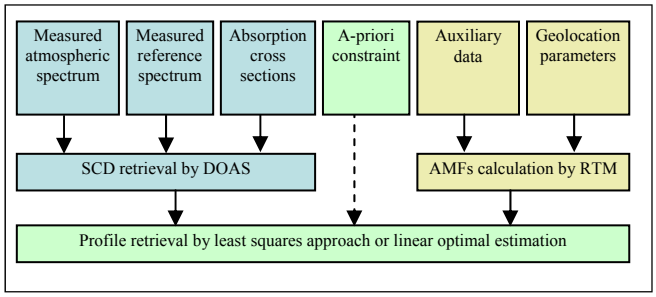

Figure 3: *Scheme of the two step approach utilizing Monte Carlo RTM Tracy II.*

3.1. First Step: Retrieval of SCDs by DOAS

For the retrieval of the OClO and BrO (also Ozone and NO_2 is retrieved) SCDs from the SCIAMACHY limb spectra, the method of Differential Optical Absorption Spectroscopy (DOAS) is used [9, 10].

This algorithm minimizes the difference between the logarithmized Fraunhofer reference and a polynomial representing scattering processes on one side and the logarithm of the measured atmospheric spectra and the sum of the absorptions due to trace gases on the other side by a least square fit. As result, the slant column densities of several trace gases absorbing in the respective wavelength range can be retrieved. The filling in of the Fraunhofer lines [23] is accounted for by a calculated Ring spectrum [22], which is handled by the fit just like the cross sections [8]. Broadband absorption and scattering is modelled by a polynomial of degree 3-5.

For the DOAS analysis, different wavelength ranges are utilized that were found to be optimal for the respective trace gas [10, 24, 25]: For OClO the fit-window ranges from 363-391 nm, for BrO from 337-357 nm, and for NO_2 from 430-450 nm. As Fraunhofer reference, the spectrum measured at a tangent height of 36 km is applied, where both OClO and BrO absorption can be regarded as negligible. For the NO_2 retrieval the reference spectrum is taken at a tangent height of 42 km.

To account for possible intensity offsets due to instrumental stray-light we include the inverse of the reference spectrum ($1/I_0$), and for the BrO retrieval also λ/I_0; similarly, for correction of polarisation features, the eta and zeta spectra taken from SCIAMACHY calibration key data are included. These additional spectra are included in the fit in the same way as the trace gas absorption cross sections. Table 1 summarizes the fit parameters for the different DOAS retrievals.
In Fig. 4 examples for the OClO and BrO DOAS analysis of selected SCIAMACHY limb spectra are shown.

Trace gas retrieval	Fit window (nm)	Included cross sections	Additional spectra	Reference Tangent height (km)
NO_2	430-450	O_3, 223 K (Bogumil et al., 2003) NO_2, 223 K (Bogumil et al., 2003) H_2O, 273 K (HITRAN) O_4 (Greenblatt et al., 1990)	Ring (Bussemer, 1993) 1/I0, eta	42-43
BrO	337-357	O_3, 223 K (Bogumil et al., 2003) O_3, 243 K (Bogumil et al., 2003) BrO (Wilmouth et al., 1999)	Ring (Bussemer, 1993) $1/I_0$, λ/I_0, eta, zeta	36-37
OClO	363-391	O_3, 223 K (Bogumil et al., 2003) NO_2, 223 K (Bogumil et al., 2003) OClO (Kromminga et al., 2003) O_4 (Greenblatt et al., 1990)	Ring (Bussemer, 1993) $1/I_0$, eta	36-37

Table 1: Wavelength ranges utilized, Cross sections and Tangent height applied as reference for the retrievals of NO_2, BrO and OClO SCDs from SCIAMACHY limb spectra.

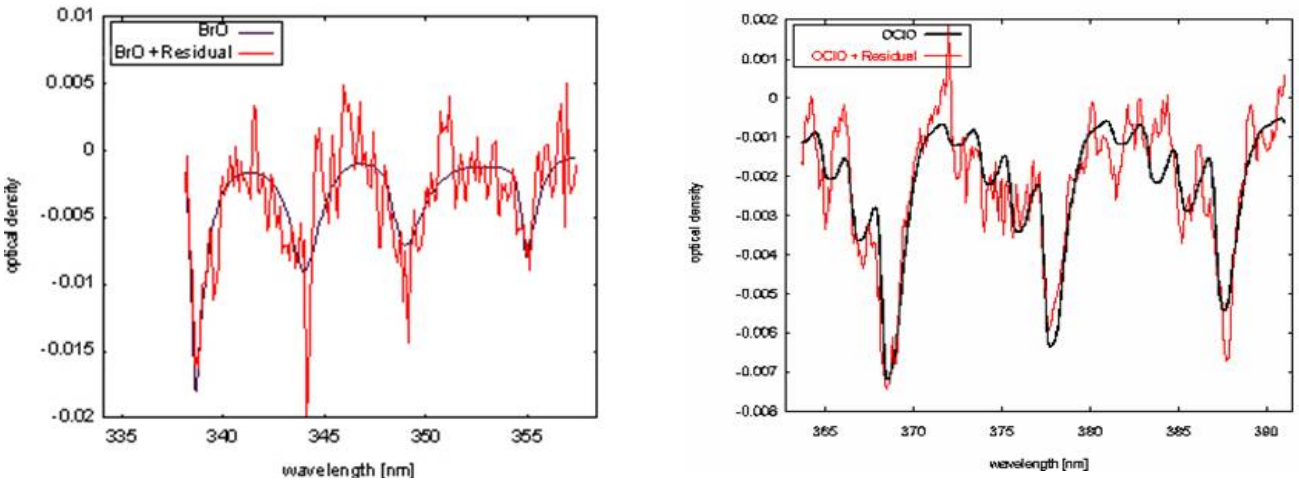

Figure 4: *Examples forDOAS analysis of SCIAMACHY limb spectra for BrO (left) and OClO (right). The black curve is the absorption structure of the respective trace gas, scaled by the SCD retrieved in the least square fit. The red curve is the black curve plus the residual, i.e. noise and structures that are not related to the spectra included in the fit.*

It can be seen that the absorption structures of the respective trace gas are found unambiguously by the DOAS fit. For OClO, the figure is an example for a situation with high chlorine activation observed at large SZA (91°), also for BrO a spectrum measured at large SZA with high optical density for BrO is evaluated. As an example for the orbit 10811 from 25th of March 2004, Fig. 5 shows BrO SCDs for different latitudes as function of the tangent height. Although these are column densities and not number densities, the figure

already reveals the differences in the abundance of BrO due to its dependence on dynamics and photochemistry: For the equator, the profile peak is at higher altitudes as for mid-latitudes and the northern polar region, reflecting the height of the Tropopause. The larger BrO abundances at high latitudes arise from the sunlight dependent conversion of the bromine reservoirs due to the suns position end of March. For altitudes above 25 km the BrO abundance is practically independent from latitude.

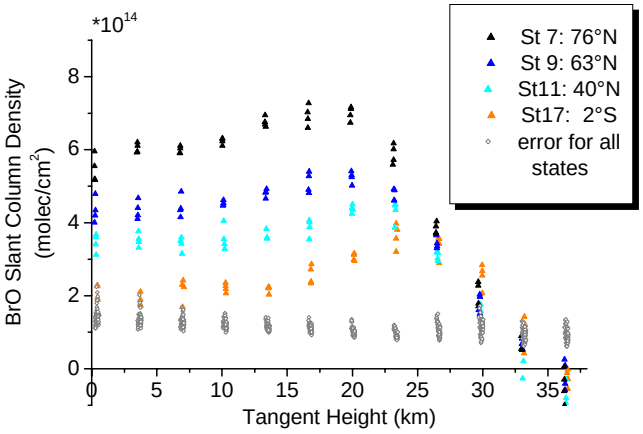

Figure 5: *BrO SCDs as function of tangent height for orbit no. 10811 from 25th of March 2004. Shown are results of the BrO DOAS retrieval for selected states at different latitudes, see legend. The grey triangles indicate the errors of the retrieval for all states of this orbit.*

3.2. Second step: Inversion of SCDs to profiles

To derive from the measured SCDs the desired trace gas profile, the physical relation between these two quantities needs to be established. For that purpose, radiative transfer is simulated by the full spherical Monte Carlo RTM "TRACY-II" [26, 27]. Applying the viewing geometry of the SCIAMACHY instrument, box air mass factors (AMF) are calculated that describe the impact of the trace gas concentration at all considered altitudes on the SCD measured for a certain tangent height. Figure 6 shows typical AMFs for BrO and OClO, revealing the impact of the different atmospheric layers (discretized as boxes with a vertical extension of 3 km) for an observation at a certain tangent height.
The matrix A_{ij} of calculated box AMFs relates the trace gas concentrations (x_j) at the different layers of the atmosphere to the measured SCDs (y_i), where ε is the error of the measurement:

$$\begin{pmatrix} y_1 \\ y_2 \\ \dots \\ y_m \end{pmatrix} = \begin{pmatrix} A_{11} & A_{12} & \dots & A_{1n} \\ A_{21} & A_{11} & \dots & A_{2n} \\ \dots & \dots & \dots & \dots \\ A_{m1} & \dots & \dots & A_{mn} \end{pmatrix} \begin{pmatrix} x_1 \\ x_2 \\ \dots \\ x_n \end{pmatrix} + \begin{pmatrix} \varepsilon_1 \\ \varepsilon_2 \\ \dots \\ \varepsilon_n \end{pmatrix} \qquad (1)$$

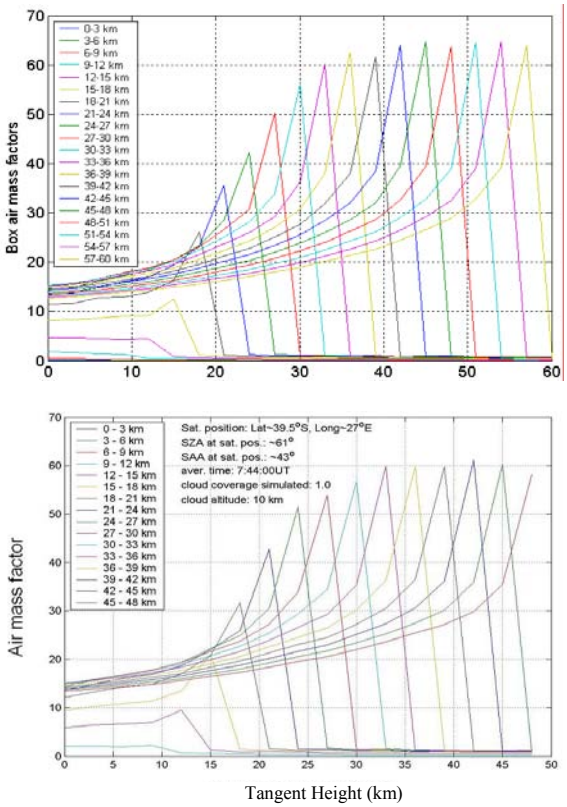

Figure 6: *Examples for Air mass factors calculated by the Monte Carlo RTM Tracy-II [26] for BrO (top) and OClO (bottom).*

To retrieve the trace gas concentration profile **x,** Eq. (1) needs to be inverted. However, the problem is not exact (the retrieved SCDs can only be measured with the error **ε**) and at the same time underdetermined (low sensitivity for the troposphere) as well as over-determined (measurements at high altitudes may be contradictory within the uncertainty). To overcome this difficulty, different approaches exist. One is to determine the profile by a least squares approach [28]:

$$\hat{x}_d = (A^T S_\varepsilon^{-1} A)^{-1} A^T S_\varepsilon^{-1} y \qquad (2)$$

where S_ε is the measurement error covariance matrix.
The inversion of the SCDs according to Eq. (2) produces reasonable results if measurements below 15 km and above 36 km are excluded, i.e. for altitudes from 15 to 36 km the problem can be treated as well-determined by the least squares approach. However, this approach is not practicable for wider altitude ranges (due to the low sensitivity for altitudes below 15 km and the decreasing signal to noise ratio for altitudes above 40 km).
Figs. 7 and 8 show examples for the inversion of BrO SCDs for two different latitudes of the orbit 10811 (compare also Fig. 5). The results for the inversion by the least squares approach (Eq. 2) are shown as blue lines in the middle panel.

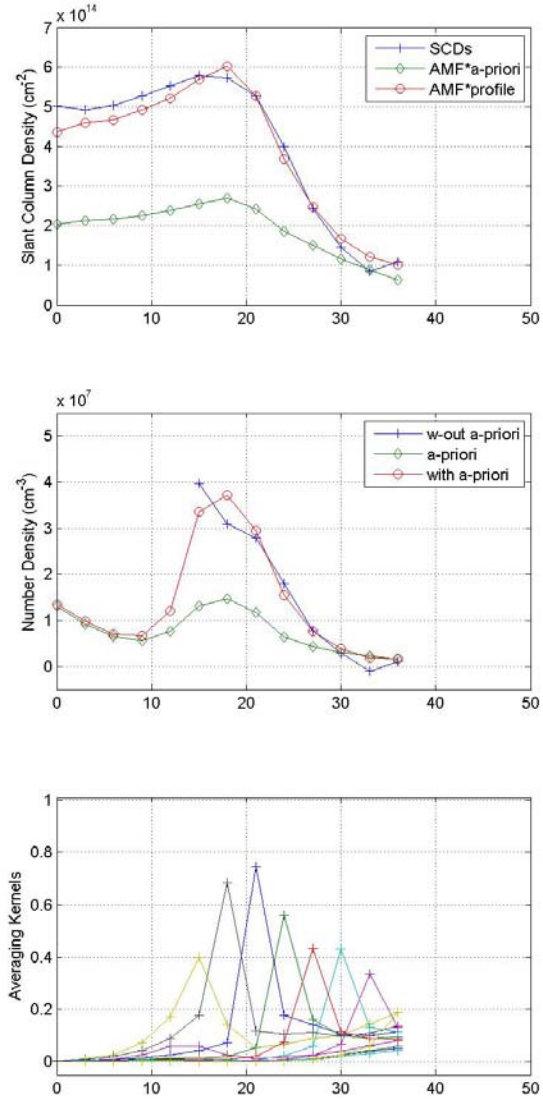

Figure 7: *BrO SCDs (top), retrieved vertical profile of number densities (middle panel) and averaging kernels for the retrieval with a priori (bottom). Values are displayed for state no. 9 (63° N) of orbit 10811.*

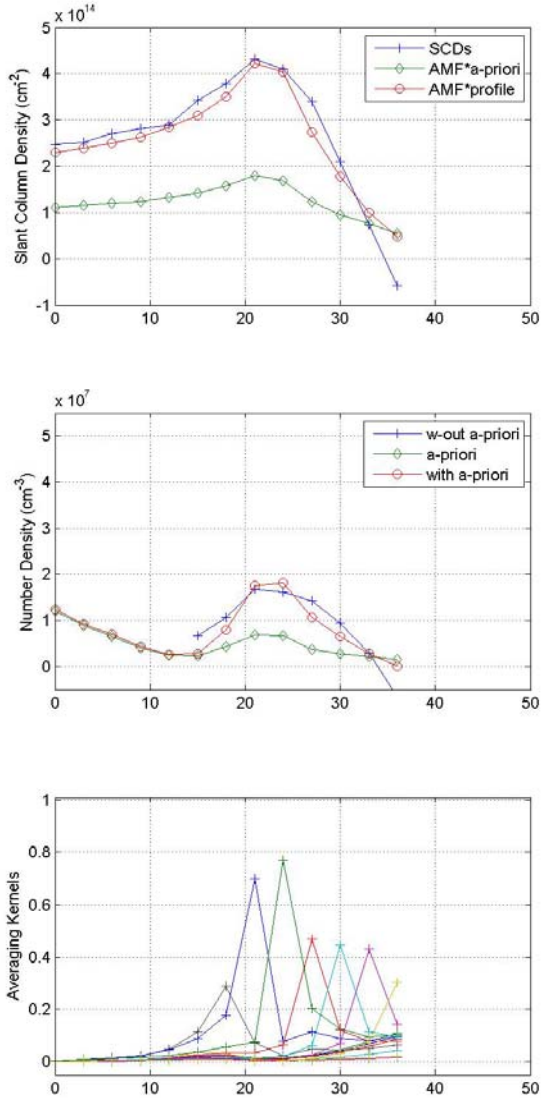

Figure 8: *same as Fig. 7 but for state no. 17 (2° S) of orbit 10811. Shown are as blue lines the measured SCDs and the profile retrieved by the least squares approach. The red lines indicate the profile retrieved by optimal estimation and the SCDs corresponding to it, applying the calculated matrix of box AMFs. The green line is the a priori profile and the SCDs corresponding to it.*

Other approaches utilize the knowledge that exists about the profile to be derived already before the measurement (e.g. climatology) as so called *a priori* information. In our case, the inversion is stabilized by an optimal estimation method (maximum a posteriori) based on [29]. For the resulting profile, the retrieved SCDs, their error covariance, the a priori profile $\mathbf{x_a}$ and its climatologic variability (described by its covariance S_a) are taken into account:

$$\boldsymbol{x} = \boldsymbol{x_a} + S_a A^T [A S_a A^T + S_y]^{-1} (\boldsymbol{y} - A\boldsymbol{x_a}) \qquad (3)$$

In Figs. 7 and 8 the BrO profiles derived by the optimal estimation approach (Eq. 3) are plotted as red lines in the middle panel.

One further result of the optimal estimation method are the so called averaging kernels (AK). They determine the altitude range where the measurement provided information on the profile: Large values indicate a large impact of the measurement, for low values of the AK the retrieved profile approaches the a priori information. The averaging kernels for the examples in Figs. 7 and 8 are shown in the bottom panel.
It can be seen that for altitudes with large AK the BrO profiles retrieved by the two approaches (with and without a priori constraint) are in good agreement.

4. BrO: COMPARISON TO BALLOON MEASUREMENTS

To investigate how well the profiles derived from applying our two step algorithm on the SCIAMACHY limb observations agree with independent, correlative measurements, we compared the BrO profiles to the ones obtained from balloon measurements performed especially for the validation of SCIAMACHY [30].
Some examples of this comparison are shown in Fig. 9. For both cases the BrO profiles agree within the error bars. There is a tendency for larger values in the SCIAMACHY BrO profiles which can be explained by the different BrO absorption cross sections utilized in the retrievals ([31] for the balloon profile retrieval, [32] for the SCIAMACHY retrieval, the latter being approx. 5-10% smaller, thus leading to larger SCDs).

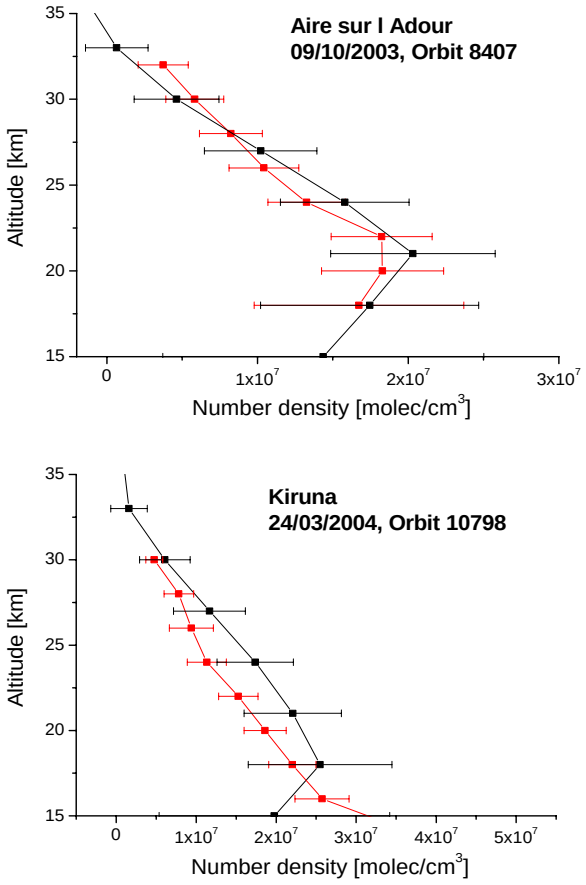

Figure 9: *BrO balloon measurements performed for SCIAMCHY validation for the 9th of October, 2003 near Aire sur l´Adour, France (top) and for the 24th of March, 2004 near Kiruna, Sweden (bottom). The balloon observations (red) are performed at the same day and correlated to the SCIAMACHY measurements (black) by trajectory calculations. Also, a photochemical correction to match the SZA of the SCIAMACHY observations has been applied [30].*

5. BrO: COMPARISON TO GROUND-BASED MEASUREMENTS

Additionally to the balloon measurements performed for the validation of SCIAMACHY, there exist correlative observations of BrO profiles by the ground-based zenith-sky DOAS retrieval [31]. Fig. 10 shows vertical concentration profiles of BrO derived by the two step approach from SCIAMACHY limb observations and from ground based measurements for Harestua (60°N, 10°E). For details on the profiling technique applied to ground-based DOAS measurements see [31, 32].
A good overall agreement is obtained in the altitude range from 15 to 25 km. However, the value at the peak (around 20 km) is usually larger in the SCIAMACHY BrO profile, which is in better agreement with the balloon measurements, see also [31].

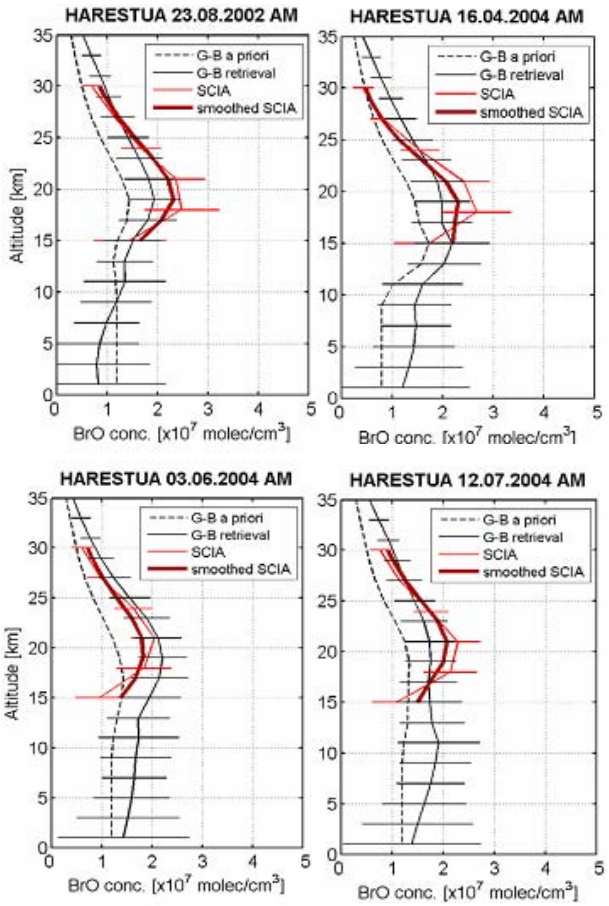

Figure 10: *Ground-based UV-visible and SCIAMACHY limb BrO profiles at Harestua for four coincidences. Due to the higher vertical resolution of the SCIAMACHY BrO profiles, they have been smoothed by convolution with the averaging kernels of the ground-based measurements to allow direct comparison [31].*

6. OClO: COMPARISON TO MEASUREMENTS OF ClO BY AURA-MLS AND ODIN-SMR

In the Arctic winters 2002/03 and 2004/05 stratospheric temperatures were well below the threshold for PSC-formation, especially in January. This caused moderate to large levels of chlorine activation, allowing to compare the SCIAMACHY OClO observations to the ones of ClO by SMR and MLS. For all examined days, the maps show a good qualitative and quantitative agreement in the level and spatial extension of chlorine activation, see Figs. 11 and 12. Deviations can be explained by the difference in the measurement time (time interval, transport inside the polar vortex).

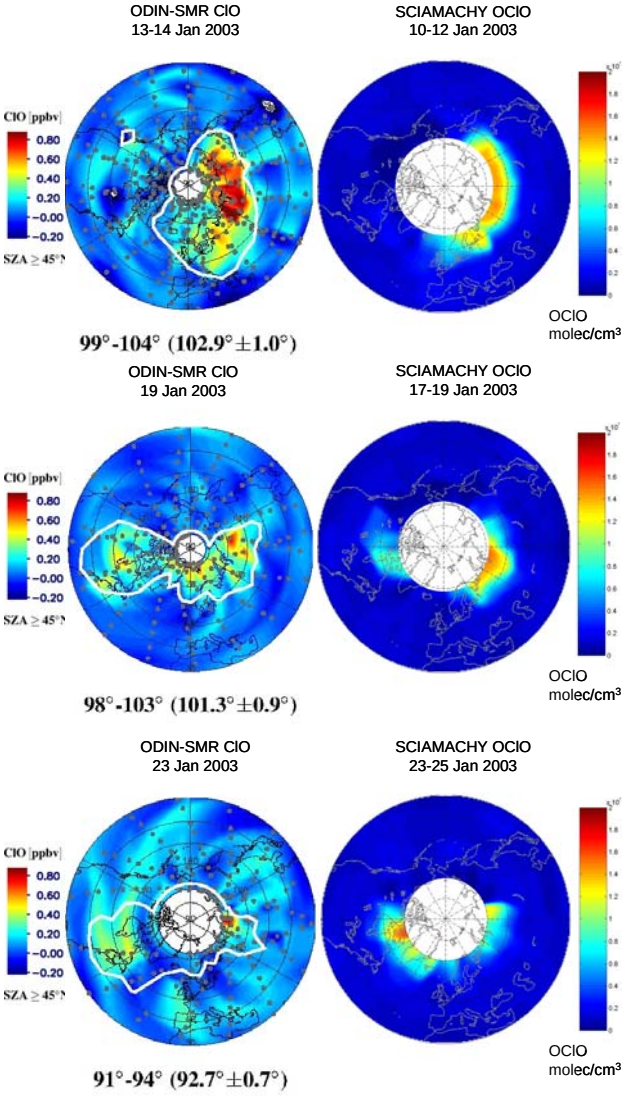

Figure 11: *OClO number density at 18 km retrieved from SCIAMACHY limb observations in comparison to the ClO mixing ratio measured by SMR (Sub Millimetre Radiometer) on ODIN at 19 km (adapted from [33]) for selected days in January, 2003. Displayed are values for the northern hemisphere in polar projection.*

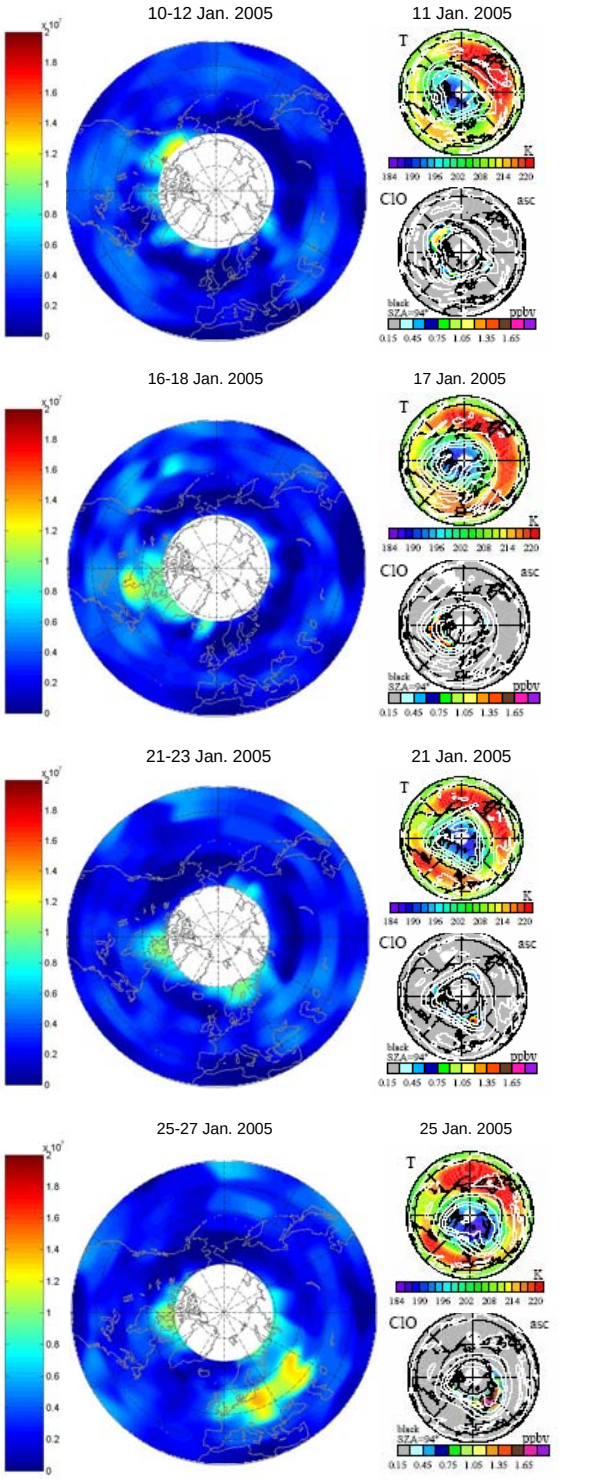

Figure 12: *OClO number density at 18 km retrieved from SCIAMACHY limb observations in comparison to the ClO mixing ratio measured by MLS (Microwave Limb Sounder) on AURA at the 490 K level (~ 18 km), taken from [34]) for selected days in January, 2005. Also shown is the temperature at the 490 K level for the northern hemisphere.*

7. HORIZONTAL GRADIENTS

The Monte Carlo RTM Tracy II contains statistical tools and a novel approach of multidimensional discretization to calculate box air mass factors (AMFs). These features might be beneficial in the profile retrieval of trace gases since it allows to account for horizontal gradients in the distribution of trace gases.

The inversion of SCDs to vertical profiles using a 2-dimensional discretization of the atmosphere will (at least to some extent) allow correcting for horizontal inhomogenities. This might be in particular important for measurements when the line of sight is crossing the polar vortex edge, but in general horizontal gradients have an impact on the profile retrieval from limb observations. Fig. 13 shows vertical profiles of OClO derived by Tracy-II RTM calculations performed either with 1-D or with 2-D discretization. It can be seen that the profiles obtained from the inversion with a 1-dim. discretization are showing larger OClO number densities and have the peak at lower altitudes. Both effects arise from horizontal gradients of the OClO abundance (generally larger values for high SZA).

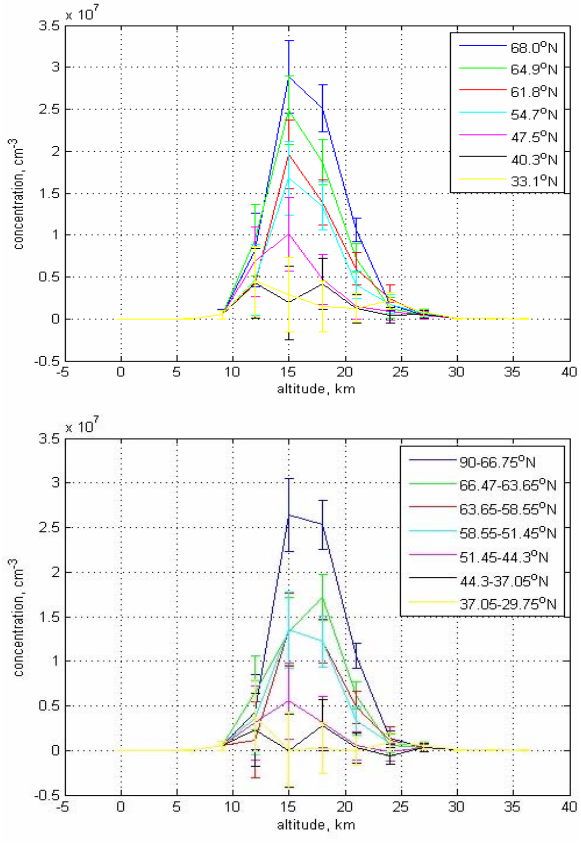

Figure 13: *Comparison of OClO profiles derived from SCIAMACHY measurements for northern latitudes either by the 1-dim inversion (top) or by accounting for horizontal gradients in the 2dim inversion (bottom). Displayed are results for orbit no. 15067 from 16th of January, 2005.*

8. CONCLUSION & OUTLOOK

Results of our two step approach for the retrieval of vertical profiles from SCIAMACHY limb observations were presented. The algorithm allows to perform the profile retrieval either with or without constraining the inversion by a priori knowledge. The inversion by the least squares approach (independently from a priori) results in reasonable profiles for altitudes between 15 and approx. 30 km. For wider altitude ranges, it is necessary to constrain the inversion by applying a priori profiles, which is achieved by the optimal estimation method.

For OClO measurements at high solar zenith angles in the northern hemisphere, the effect of horizontal gradients on the profile retrieval was investigated by utilizing either a 1-dim. or 2-dim. discretization of the atmosphere. It was found that the inversion applying a 2-dim. discretization can to some extent correct for inhomogenities in the trace gas distribution.

Results for BrO and OClO profiles were compared to balloon and ground-based validation measurements as well as satellite observations. For all comparison studies performed, a good agreement was found. However, the number of correlated measurements is small (for OClO none exist so far).

After further validation and sensitivity studies, the complete record of SCIAMACHY limb spectra (since October 2002 until present) will be evaluated for NO_2, BrO and OClO profiles. The obtained data set of vertical profiles will be applied for studies on stratospheric chemistry, like inter-annual and inter-hemispheric comparisons (variability and evolution of the magnitude and profile peak height), correlations to stratospheric temperatures and other stratospheric trace gases, and comparison to results from established model simulations.

For BrO and OClO it may be possible to improve the profile retrieval if the diurnal cycle is accounted for. This is in particular important for limb measurements close to the terminator, where the abundance of BrO and OClO is strongly depending on the SZA. In this respect, it will be useful to complete the daytime OClO profiles derived from limb observations with the night-time OClO profiles from SCIAMACHY occultation measurements.

9. ACKNOWLEDGMENTS

We thank Joachim Urban (Chalmers University, Göteborg) for the ODIN-SMR observations of ClO.

We are grateful to the AURA MLS team (JPL) for providing the MLS ClO measurements via their website.

We wish to thank Alexei Rozanov, IUP Bremen, for fruitful discussions regarding the retrieval of BrO profiles.

10. REFERENCES

1. Solomon, S. (1999), Stratospheric Ozone Depletion: A Review of Concepts and History, *Reviews of Geophysics, 37*(3), 275-316, 1999.

2. Molina, L.T. and M.J. Molina, Production of Cl_2O_2 from the self reaction of the ClO radical, *J. Chem. Phys., 91,* 433-436, 1987.

3. Mc Elroy, M.B., R.J. Salawitch, S.C. Wofsy and J.A. Logan, Reductions of Antarctic ozone due to synergistic interactions of chlorine and bromine, *Nature, 321,* 759-762, 1986.

4. Toumi, R., Reaction of ClO with NO_3: OClO formation and night-time O_3 loss, *Geophys. Res. Lett., 21*(13), 1487-1490, 1994.

5. Schiller, C. and A. Wahner, Comment on 'Stratospheric OClO Measurements as a poor quantitative indicator of chlorine activation' by J. Sessler, M.P. Chipperfield, J.A. Pyle and R. Toumi, *Geophys. Res. Lett., 23,* 1053-1054, 1996.

6. Sessler, J., M.P. Chipperfield, J.A. Pyle and R. Toumi, Reply to Schiller, C. and A. Wahner (1996), *Geophys. Res. Lett., 23,* 1055, 1996.

7. Tornkvist, K.K., D.W. Arlander and B.-M. Sinnhuber, Ground-Based UV Measurements of BrO and OClO over Ny-Alesund during Winter 1996 and 1997 and Andoya during Winter 1998/99, *J. Atm. Chem., 43,* 75-106, 2002.

8. Solomon, S., G.H. Mount, R.W. Sanders and A.L. Schmeltekopf, Visible Spectroscopy at McMurdo Station, Antarctica 2. Observations of OClO, *J. Geophys. Res., 92,* 8329-8338, 1987.

9. Platt, U., Differential Optical Absorption Spectroscopy (DOAS), in *Air Monitoring by Spectroscopic Techniques*, edited by M. W. Sigrist, Chemical Analysis Series Vol. 127, John Wiley, New York, 1994.

10. Wagner, T., C. Leue, K. Pfeilsticker and U. Platt, Monitoring of the stratospheric chlorine activation by Global Ozone Monitoring Experiment (GOME) OClO measurements in the austral and boreal winters 1995 through 1999, *J. Geophys. Res., 106,* 4971-4986, 2001.

11. Wagner, T., F.Wittrock, A. Richter, M.Wenig, J.P. Burrows, and U. Platt, Continuous monitoring of the high and persistent chlorine activation during the Arctic winter 1999/2000 by the GOME instrument on ERS-2, *J. Geophys. Res.*, *107*(D20), 8267, doi : 10.1029/2001JD000466, 2002.

12. Kühl, S., W. Wilms-Grabe, et al. and T. Wagner, Stratospheric Chlorine Activation in the Arctic winters 1995/96 to 2001/02 derived from GOME OClO Measurements, *Adv. Space Res.*, *34*, 798-803, 2004.

13. Weber, M., S. Dhomse, F. Wittrock, A. Richter, B.-M. Sinnhuber and J.P. Burrows, Dynamical control of NH and SH winter/spring total ozone from GOME observations in 1995-2002, *Geophys. Res. Lett.*, *30*(1), doi: 10.1029/ 2002GL016008, 2003.

14. Richter, A., F. Wittrock, M. Weber, S. Beirle, S. Kühl, U. Platt, T. Wagner, W. Wilms- Grabe and J.P. Burrows (2004), GOME observations of stratospheric trace gas distributions during the splitting vortex event in the Antarctic winter 2002 Part I: Measurements, *J. Atm. Sci.*, *62*, 778-785, 2005.

15. Kühl, S., A. Dörnbrack, W. Wilms-Grabe, B.-M-Sinnhuber, U. Platt and T. Wagner, Observational evidence for rapid chlorine activation by mountain waves above Northern Scandinavia, *J. Geophys. Res*, *109*, D22309, doi:10.1029/2004JD004797, 2004.

16. Bovensmann, H., J. P. Burrows, M. Buchwitz, J. Frerick, S. Noël, V. V. Rozanov, K. V. Chance, and A. H. P. Goede, SCIAMACHY - Mission objectives and measurement modes, *J. Atmos. Sci.*, *56*, (2), 127-150, 1999.

17. Burrows, J.P. et al., The Global Ozone Monitoring Experiment (GOME): Mission Concept and First Scientific Results, *J. Atmos. Sci.*, *56,* 151-175, 1999.

18. Kromminga, H., J. Orphal, P. Spietz, S. Voigt and J.P. Burrows, New measurements of OClO absorption cross sections in the 325-435 nm and their temperature dependence between 213-293 K, *J. Photochem. Photobiol. A.: Chemistry*, *157*, 149-160, 2003.

19. Bogumil, K., J. Orphal, T. Homann, S. Voigt, P.Spietz, O.C. Fleischmann, A. Vogel, M. Hartmann, H. Bovensmann, J. Frerik and J.P. Burrows, Measurements of Molecular Absorption Spectra with the SCIAMACHY Pre-Flight Model: Instrument Characterization and Reference Data for Atmospheric Remote-Sensing in the 230-2380 nm Region, *J. Photochem. Photobiol. A.*, *157*, 167-184, 2003.

20. Greenblatt, G. D., J. J. Orlando, J. B. Burkholder, and A. R. Ravishankara, Absorption measurements of oxygen between 330 and 1140nm, *J. Geophys. Res.*, 95: 18577-18582, 1990.

21. Vandaele, A. C., C. Hermans, P. C. Simon, M. Carleer, R. Colin, S. Fally, M.-F. Mérienne, A. Jenouvrier, and B. Coquart, Measurements of the NO_2 Absorption Cross-section from 42000 cm-1 to 10000 cm-1 (238-1000 nm) at 220 K and 294 K, J. Quant. Spectrosc. Radiat. Transfer, 59, 171-184, 1997.

22. Bussemer, M., Der Ring-Effekt: Ursachen und Einfluß auf die Messung stratospärischer Spurenstoffe, *Diploma Thesis, University of Heidelberg,* 1993.

23. Grainer, J.F. and J. Ring, Anomalous Fraunhofer line profiles, *Nature*, *193*, 1962.

24. Wagner, T., Satellite observations of Atmospheric Halogen oxides, PhD thesis, University of Heidelberg, 1999.

25. Kühl, S., Quantifying Stratospheric chlorine chemistry by the satellite spectrometers GOME and SCIAMACHY, PhD Thesis, Universität Heidelberg, 2005.

26. Deutschmann, T., T. Wagner, C. von Friedeburg, TRACY-II Manual, Universität Heidelberg, 2006.

27. Wagner, T., et al., Comparison of Box-Air-Mass-Factors and Radiances for Multiple-Axis Differential Optical Absorption Spectroscopy (MAX-DOAS) Geometries calculated from different UV/visible Radiative Transfer Models, *Atmos. Chem. Phys. Discuss.*, *6*, 9823-9876, 2006.

28. Menke, W., Geophysical data analysis: discrete inverse theory, Academic Press, 1999.

29. Rodgers, C.D., Inverse methods for atmospheric sounding. Theory and practice, World Scientific Publishing Co. Ltd., Singapore, 2000.

30. Dorf, M., et al., Balloon-borne stratospheric BrO measurements: comparison with Envisat / SCIAMACHY BrO limb profiles, *Atmos. Chem. Phys.*, *6*, 2483-2501, 2006.

31. Hendrick, F., et al., BrO Profiling from ground-based DOAS observations: New tool for the ENVISAT/SCIAMACHY Validation, *Proceedings of the ESA Atmospheric Science Conference*, Frascati, 2006: http://earth.esa.int/atmos2006/

32. Hendrick, F., et al., Retrieval of nitrogen dioxide stratospheric profiles from ground-based zenith-sky UV-visible observations: validation of the technique through correlative comparisons, *Atmos. Chem. Phys.*, *4*, 2091–2106, 2004.

33. Urban, J., N. Lautie et al., The northern hemisphere stratospheric vortex during the 2002-03 winter: Subsidence, chlorine activation and ozone loss observed by the Odin Sub-Millimetre Radiometer, *Geophys. Res. Letts.*, *31*, doi: 10.1029/2003GL019089, 2004.

34. JPL-MLS webpage: http://mls.jpl.nasa.gov/data